Journal of Computational Electronics 3: 263–267, 2004

Local Discontinuous Galerkin Methods for Moment Models in Device Simulations: Formulation and One Dimensional Results

YUNXIAN LIU
School of Mathematics and System Sciences, Shandong University, Jinan, Shandong 250100, China
yxliu@sdu.edu.cn

CHI-WANG SHU
Division of Applied Mathematics, Brown University, Providence, RI 02912, USA
shu@dam.brown.edu

Abstract. We report our preliminary work in applying the local discontinuous Galerkin (LDG) finite element method to solve time dependent and steady state moment models, such as the hydrodynamic (HD) models and the energy transport (ET) models, for semiconductor device simulations, in which both the first derivative convection terms and second derivative diffusion (heat conduction) terms exist and are discretized by the discontinuous Galerkin (DG) method and the LDG method respectively. The potential equation for the electric field is also discretized by the LDG method, thus the numerical tool is based on a unified discontinuous Galerkin methodology for different components and is hence potentially viable for efficient h-p adaptivity and parallel implementation. One dimensional n^+-n-n^+ diode is simulated in this paper using the HD and ET models and comparison is made with earlier finite difference Essentially Non-Oscillatory (ENO) simulation results.

Keywords: discontinuous Galerkin method, adaptivity, hydrodynamic model, energy transport model

1. Introduction

In this paper we report our preliminary work in applying the local discontinuous Galerkin (LDG) finite element method to solve various time dependent and steady state moment models for semiconductor device simulations, in which both the first derivative convection terms and second derivative diffusion (heat conduction) terms exist and are discretized by the discontinuous Galerkin (DG) method and the LDG method [3,4] respectively. The potential equation for the electric field is also discretized by the LDG method. This is an ongoing project with the objective of developing a numerical tool based on the DG and LDG methodology, capable of solving various models for semiconductor device simulations (hydrodynamic (HD) models, energy transport (ET) models, quantum drift-diffusion or quantum hydrodynamic models, kinetic models, etc.) in a unified treatment of first and higher spatial derivatives, including those for the potential equations, which would allow easy h-p adaptivity and efficient parallel implementation.

The discontinuous Galerkin method is a finite element method which uses discontinuous piecewise polynomials as basis functions and relies on an adequate choice of numerical fluxes, which handle effectively the interactions across element boundaries, to achieve stable and accurate algorithms for nonlinear hyperbolic conservation laws (those involving first spatial derivatives), nonlinear convection diffusion equations (those involving first and second spatial derivatives), nonlinear dispersive equations (those involving first, second, and third spatial derivatives), etc., see for example [3,7] and the review paper [4] and references therein. The discontinuous Galerkin method was used before for semiconductor device simulations, such as in [2] for

the hydrodynamic models and in [1] for the quantum-hydrodynamic models, however in these earlier works only the convective terms were discretized by the discontinuous Galerkin methodology. Recent development of the locally discontinuous Galerkin method in treating higher order spatial derivatives allows us to adopt a unified discretization strategy to handle all spatial derivatives in these models, thus allowing the full usage of the potential of this methodology in easy h-p adaptivity and parallel efficiency.

In Section 2 we will describe briefly two moment models (ET and HD models) that we use to test the numerical method. In Section 3 we will describe briefly the LDG method using the ET model as an example. Section 4 contains numerical results on a one dimensional n^+-n-n^+ diode to demonstrate the numerical method. We mention a plan for future work at the end of Section 4.

2. One Dimensional ET and HD Models

In this section, we briefly describe two one-dimensional moment models of semiconductor devices: the ET model and the HD model, that we will use for testing the numerical method. We follow the description in [5] and refer to [5] and the references therein for more details.

2.1. The ET Model

The ET model is described by

$$u_t + f(u)_x = g(u)_{xx} + h(u) \tag{1}$$

where

$$\begin{cases} u = \left(en, \dfrac{nE}{m}\right), \\ f(u) = \phi_x n(e\mu(E), \mu^E(E) + D(E)), \\ g(u) = (nD(E), nD^E(E)), \\ h(u) = (0, en\mu(E)(\phi_x)^2 + \dfrac{e}{\varepsilon}(n - n_d)nD(E) - nE_c \end{cases}$$

and the electric field $-\phi_x$ is obtained from the Poisson equation

$$\phi_{xx} = \frac{e}{\varepsilon}(n - n_d). \tag{2}$$

Here, the electron concentration n, the energy E, and the electric potential ϕ are the unknown variables. e, m, ε and n_d are given constants or functions, representing the electron charge modulus, the effective electron mass, the dielectric permittivity and the doping, respectively. The mobilities μ and μ^E are given by

$$\mu = \mu_0 \frac{T_0}{T}, \quad \mu^E = \frac{3}{2}\mu_0 k T_0 \left(1 - \frac{5kT}{4e}\right),$$

the diffusion coefficients D and D^E are given by

$$D = k\mu_0 T_0, \quad D^E = \frac{3}{2e}\mu_0 k^2 T_0 T \left(1 - \frac{5kT}{4e}\right),$$

and the collision term E_c is given by

$$E_c = \frac{15k}{4}\left[\left(1 + \frac{1}{2}\frac{k}{e}T\right)T - T_0\right],$$

where T_0 is the constant lattice temperature, and the temperature T is related to the energy E by

$$E = \frac{3}{2}kT\left(1 + \frac{5}{4}kT\right).$$

Here k is the Boltzmann constant.

2.2. The HD Model

The HD model is described by the following equations

$$\begin{cases} n_t + (nv)_x = 0, \\ p_t + (pv + knT)_x = en\phi_x - \dfrac{p}{\tau_p}, \\ W_t + (v(W + knT))_x = env\phi_x + (\kappa T_x)_x - \dfrac{W - W_0}{\tau_w}. \end{cases} \tag{3}$$

where the electric field $-\phi_x$ is again obtained from the Poisson Eq. (2). In this model, n still represents the electron concentration, v is the velocity, W is the total energy. The momentum p is related to v by $p = mnv$, and the temperature T is related to the total energy W by

$$W = \frac{3}{2}knT + \frac{1}{2}mnv^2.$$

The momentum and energy relaxation times are given by $\tau_p = C_p \frac{T_0}{T}$ and $\tau_w = C_w \frac{T}{T+T_0} + \frac{1}{2}\tau_p$, where C_p

and C_w are constants. κ is the thermal conductivity governed by the Wiedemann-Franz law, described by $\kappa = \frac{3}{2} n \frac{k^2 \mu_0 T_0}{e}$.

3. The LDG Method

In this section, we briefly describe the LDG method, using the ET model (1)–(2) as an example. For more details of the DG and LDG methods, including stability analysis and error estimates, we refer to [3,4,7] and the references therein. The starting point of the LDG method is to rewrite PDEs containing higher order spatial derivatives as a larger system containing only first order spatial derivatives. Thus the ET model (1)–(2) is rewritten as

$$\begin{cases} u_t + (f(u) - q)_x = h(u), \\ q - g(u)_x = 0, \\ r_x = \dfrac{e}{\varepsilon}(n - n_d), \\ r - \phi_x = 0. \end{cases} \tag{4}$$

Let $I_j = (x_{j-1/2}, x_{j+1/2})$, $j = 1, 2, \cdots, N$ be a partition of the computational domain, $\Delta x_j = x_{j+1/2} - x_{j-1/2}$, $h = \sup_j \Delta x_j$ and $x_j = \frac{1}{2}(x_{j-1/2} + x_{j+1/2})$. The finite dimensional computational space is

$$V_h = V_h^k = \{z : z \mid I_j \in P^k(I_j)\}$$

where $P^k(I_j)$ denotes the set of polynomials of degree up to k defined on I_j. Both the numerical solution and the test functions will come from this space V_h^k. Notice that both the mesh sizes Δx_j and the degree of polynomials k can be changed from element to element freely, thus allowing for easy h-p adaptivity. Different choices of bases for V_h^k do not alter the algorithm. We choose locally orthogonal scaled Legendre polynomials basis over $I_j = (x_{j-1/2}, x_{j+1/2})$ for our implementation:

$$v_0^{(j)}(x) = 1,\ v_1^{(j)}(x) = \xi(x),\ v_2^{(j)}(x) = \xi^2(x) - \frac{1}{12}, \cdots.$$

where $\xi(x) = \frac{x - x_j}{\Delta x_j}$. The numerical solution can then be written as $u^h(x, t) = \sum_{l=0}^{k} u_j^{(l)}(t) v_l^{(j)}(x)$ for $x \in I_j$.

We multiply each Eq. (4) by a test function $z \in V_h^k$, integrate over I_j, formally integrate by parts for all terms involving a spatial derivative, replace the exact solution u, q, r and ϕ by their numerical approximations u^h, q^h, r^h and ϕ^h in V_h^k, and replace terms on the cell boundaries by suitable numerical fluxes to obtain the LDG scheme:

$$\begin{cases} \displaystyle\int_{I_j} (u^h)_t z dx - \int_{I_j} (f(u^h) - q^h) z_x dx \\ \quad + (\hat{f}(u^h) - \hat{q}^h)_{j+1/2} z_{j+1/2}^- \\ \quad - (\hat{f}(u^h) - \hat{q}^h)_{j-1/2} z_{j-1/2}^+ = \displaystyle\int_{I_j} h(u^h) z dx, \\ \displaystyle\int_{I_j} q^h z dx + \int_{I_j} g(u^h) z_x dx - \hat{g}(u^h)_{j+1/2} z_{j+1/2}^- \\ \quad + \hat{g}(u^h)_{j-1/2} z_{j-1/2}^+ = 0, \\ \displaystyle - \int_{I_j} r^h z_x dx + \hat{r}_{j+1/2}^h z_{j+1/2}^- - \hat{r}_{j-1/2}^h z_{j-1/2}^+ \\ \quad = \displaystyle\int_{I_j} \frac{e}{\epsilon}(n^h - n_d) z dx, \\ \displaystyle\int_{I_j} r^h z dx - \hat{\phi}_{j+1/2}^h z_{j+1/2}^- + \hat{\phi}_{j-1/2}^h z_{j-1/2}^+ \\ \quad + \displaystyle\int_{I_j} \phi^h z_x dx = 0 \end{cases} \tag{5}$$

where, e.g. $z_{j+1/2}^- = z(x_{j+1/2}^-)$. The "hat" terms are the numerical fluxes which are chosen as follows: $\hat{f}(u^h)$ in the first Eq. (5) is chosen as the Lax-Friedrichs flux, see, e.g. [4] and the references therein. $\hat{q}^h$ in the first equation and $\hat{g}(u^h)$ in the second equation are chosen as the "alternate" fluxes $\hat{q}^h = (q^h)^-$ and $\hat{g}(u^h) = g((u^h)^+)$ (the "$-$" and "$+$" can also be reversed), see [3]. Notice that the auxiliary variable q^h can be locally solved from the second Eq. (5) and substituted into the first equation. This is the reason the method is called the "local" discontinuous Galerkin method and this also distinguishes LDG from the classical mixed finite element methods, where the auxiliary variable q^h must be solved from a global system. In the third and fourth Eq. (5), which discretize the Poisson equation, we choose numerical flux $\hat{r}^h$ and $\hat{\phi}^h$ as $\hat{\phi}^h = (\phi^h)^-$, $\hat{r}^h = (r^h)^+ - [\phi^h]$ (the "$-$" and "$+$" can also be reversed), where $[\phi^h]$ denotes the jump $(\phi^h)^+ - (\phi^h)^-$. Again, the auxiliary variable r^h can be locally solved from the fourth Eq. (5) and substituted into the third equation, resulting in a system for ϕ^h which can be solved by standard linear solvers. Noticed that the Poisson equation is coupled to the first Eq. (5) through the $h(u^h)$ term, which contains r^h. The first Eq. (5) is advanced with the third order total variation diminishing (TVD) Runge-Kutta method [6] in time, until a steady state is reached for our steady state diode test case.

4. Numerical Results

In this section we demonstrate the LDG method by a numerical example for a one dimensional n^+-n-n^+

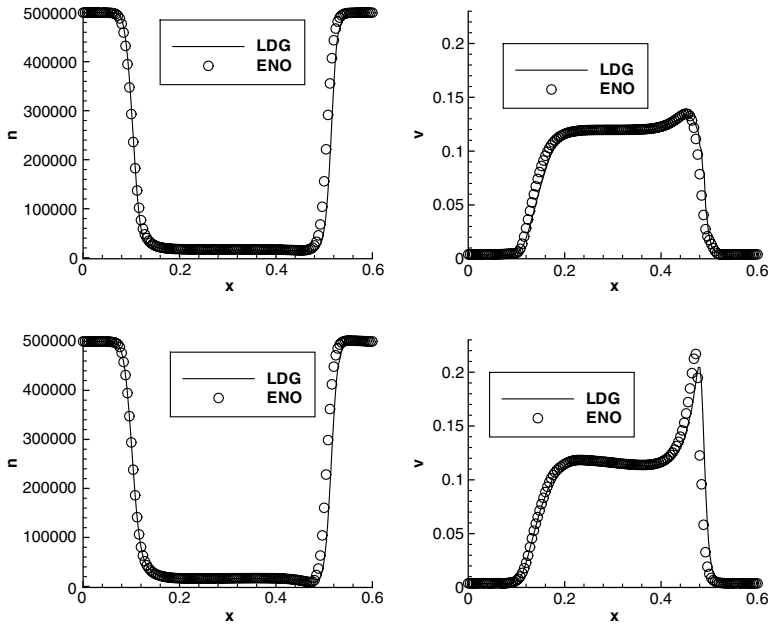

Figure 1. Comparison of the LDG method (solid lines) with the finite difference ENO method (symbols). ET model (top) and HD model (bottom). Left: electron density n (10^{12} cm^{-3}); right: velocity v (μ m/ps).

diode using the ET model (1)–(2) and the HD model (3)–(2). The silicon diode we simulate has a length of 0.6 μm with a doping defined by $n_d = 5 \times 10^{17}$ cm^{-3} in $[0, 0.1]$ and in $[0.5, 0.6]$ and $n_d = 2 \times 10^{15}$ cm^{-3} in $[0.15, 0.45]$, with a smooth transition in between. The lattice temperature is taken as $T_0 = 300^\circ$K. The constants C_p and C_w in the relaxation times τ_p and τ_w are given by $C_p = \frac{m}{e}\mu_0, C_w = \frac{3\mu_0 k T_0}{2e v_s^2}$ with $k = 0.138\times 10^{-4}, e = 0.1602, m = 0.26\times 0.9109\times 10^{-31} kg, \mu_0 = 0.14$ for the HD model and $\mu_0 = 0.0088(1 + \frac{14.2273}{1+\frac{n_d}{143200}})$ in the ET model, and $v_s = 0.1$, in our units.

The boundary conditions are given as follows: $\phi = \phi_0 = \frac{kT}{e}\ln(\frac{n_d}{n_i})$ at the left boundary, with $n_i = 1.4 \times 10^{10}$ cm^{-3}, $\phi = \phi_0 + vbias$ with the voltage drop $vbias = 1.5$ at the right boundary for the potential; $T = 300^\circ$K at both boundaries for the temperature; $n = 5 \times 10^{17}$ cm^{-3} at both boundaries for the concentration; and Neumann boundary condition is used for the velocity v at both boundaries.

First, we show the results of the comparison between the second order LDG method (piecewise linear $k = 1$) and the third order ENO finite difference method [5] using 150 uniform cells in Fig. 1 We can clearly see that the LDG method provides very good numerical results in agreement with the results obtained by the ENO finite difference method.

Next we compare the simulation results of the LDG method using a uniform mesh with 150 cells (we denote its cell size by Δx_1) and a non-uniform mesh with 75 cells. The non-uniform mesh has two distinct mesh sizes, Δx_1 in the two intervals $[0.05, 0.15]$ and $[0.45, 0.55]$ near the junctions, and $\Delta x_2 = 4\Delta x_1$ for the remaining part of the domain. The comparison is given in Fig. 2.

We can clearly see from Fig. 2 that the LDG method with a non-uniform, coarser mesh and with a uniform mesh with more cells has comparable resolutions, provided that they have the same mesh size near the critical junction regions. Notice that many numerical schemes have difficulties in handling abrupt changes in mesh sizes in adjacent cells, however the LDG method is designed to handle such meshes with full stability and accuracy. This advantage of the LDG method in handling arbitrary meshes will be more apparent in two dimensional simulations.

For this ongoing project, future work will include generalization to two dimensional problems and to other models of device simulations.

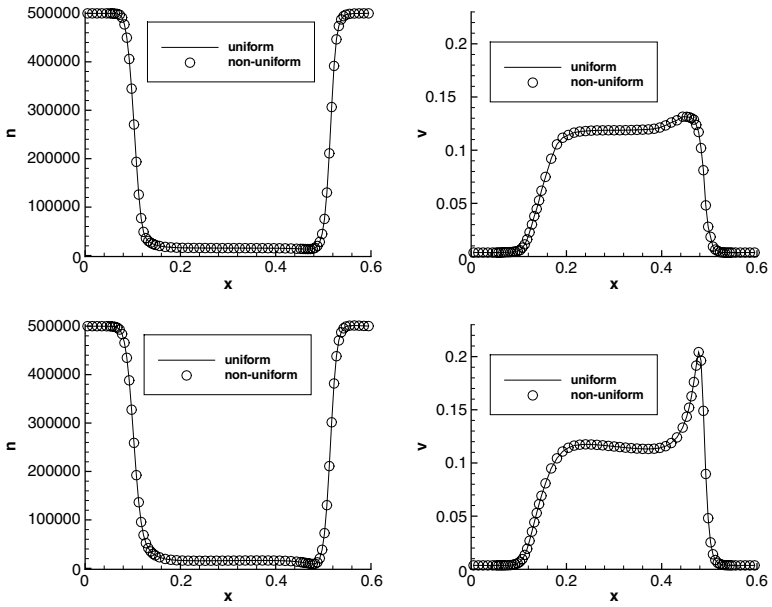

Figure 2. LDG method. Comparison between a uniform mesh with 150 cells (solid lines) and a non-uniform mesh with 75 cells (symbols). ET model (top) and HD model (bottom). Left: electron density n (10^{12} cm^{-3}); right: velocity v (μm/ps).

Acknowledgments

The research of Y. Liu is partially supported by NNSF grants 10372052, 10271066 and DFME grant 20030422047 of China. The research of C.-W. Shu is partially supported by ARO grant W911NF-04-1-0291 and NSF grant DMS-0207451.

References

1. Z. Chen, B. Cockburn, C. Gardner, and J. Jerome, "Quantum hydrodynamic simulation of hysteresis in the resonant tunneling diode," *J. Comput. Phys.*, **117**, 274 (1995).
2. Z. Chen, B. Cockburn, J. Jerome, and C.-W. Shu, "Mixed-RKDG finite element methods for the 2-D hydrodynamic model for semiconductor device simulation," *VLSI Design*, **3**, 145 (1995).
3. B. Cockburn and C.-W. Shu, "The local discontinuous Galerkin method for time-dependent convection-diffusion systems," *SIAM J. Numer. Anal.*, **35**, 2440 (1998).
4. B. Cockburn and C.-W. Shu, "Runge-Kutta Discontinuous Galerkin methods for convection-dominated problems," *J. Sci. Comput.*, **173**, 145 (2001).
5. J. Jerome and C.-W. Shu, "Energy models for one-carrier transport in semiconductor devices problems," in *IMA Volumes in Mathematics and Its Applications*, Volume 59, edited by W. Coughran, J. Cole, P. Lloyd, and J. White (Springer-Verlag, Berlin, 1994) p. 185.
6. C.-W. Shu and S. Osher, "Efficient implementation of essentially non-oscillatory shock-capturing schemes," *J. Comput. Phys.*, **77**, 439 (1988).
7. J. Yan and C.-W. Shu, "A local discontinuous Galerkin method for KdV type equations," *SIAM J. Numer. Anal.*, **40**, 769 (2002).